

Synthesis, Structure, and Characterization of N-Ligated Tungsten Selenide Cluster Complexes $W_6Se_8L_6$

Xiaobing Xie and Robert E. McCarley*

Ames Laboratory, USDOE, and Department of Chemistry, Iowa State University, Ames, Iowa 50011

Received May 25, 1995[⊗]

Two new W_6Se_8 cluster units are reported via the reaction of W_6Cl_{12} with Na_2Se in the refluxing amine solvents pyridine (py) and piperidine (pip). Crystals for both complexes were grown from the reaction filtrates. Crystallographic data for these complexes are as follows: $W_6Se_8(pip)_6 \cdot 8pip$ (**1**), cubic, $I\bar{4}3d$, $a = 31.150(4)$ Å, $Z = 12$; $W_6Se_8(py)_6 \cdot 6py$ (**2**), trigonal, $R\bar{3}$, $a = 19.654(2)$ Å, $c = 15.100(5)$ Å, $Z = 3$. W–W and W–Se bond distances show little variation among the complexes with average values of 2.691(1) and 2.574(1) Å, respectively. Photoelectron spectra give characteristic tungsten binding energies at 30.8 eV ($W 4f_{7/2}$) and 32.9 eV ($W 4f_{5/2}$). IR spectra show strong bands at 243–254 cm^{-1} , attributable to the T_{1u} W–Se stretching modes.

Introduction

The synthesis of tungsten chalcogenide cluster complexes, $W_6Y_8L_6$ ($Y = S, Se, Te$; $L =$ donor ligand) and their possible conversion into the ternary compounds $M_xW_6Y_8$, has become a major scientific goal. This attention is derived from the relation of these compounds to the well-known Chevrel phases, $M_xMo_6Y_8$, which exhibit a range of interesting physical and chemical properties, including those of superconductors with high H_{c2} ,¹ ordered magnetic phases,² solid electrolytes (fast ion conductors),³ and hydrodesulfurization (HDS) catalysts.⁴ The essential structural elements in these Chevrel phase compounds are the Mo_6Y_8 units with octahedral Mo_6 clusters which have variable electron populations of 20–24 electrons in the Mo–Mo bonding orbitals. The production of the Chevrel phases has generally involved solid-state reactions at higher temperatures (1000–1300 °C).

In contrast to the abundance of these molybdenum compounds, no example of the tungsten analogues, W_6Y_8 or $M_xW_6Y_8$, has been reported. It is generally understood that these compounds cannot be obtained at high temperatures because they are unstable with respect to disproportionation (into W and WY_2 or W, WY_2 , and $MY_{n/2}$, where n is the valence of M). Thus, these metastable phases may exist only at lower temperatures, where the thermodynamic equilibrium can be avoided. We have initiated research toward preparation of these tungsten analogues at low temperatures through molecular precursors. The conversion of W_6Cl_{12} , which contains the $(W_6Cl_8)^{4+}$ cluster unit, by sulfide substitution was successfully accomplished without cluster decomposition.^{5–7} The preparation and structural characterization of $W_6S_8L_6$ molecular complexes, where L is an organic donor ligand such as pyridine,⁵ piperidine,⁶ triethylphosphine,⁷ or tetrahydrothiophene,⁷ were accomplished in this laboratory. Likewise, the molybdenum

sulfide cluster complexes, $Mo_6S_8L_6$, were also developed.⁸ Concurrently, a low-yield synthesis of $W_6S_8(PEt_3)_6$ via “reductive dimerization” of a complex formed between $W_3S_7Cl_4$ and triethylphosphine was reported by Saito *et al.*⁹

However, no example of either the tungsten selenide or the tungsten telluride molecular complexes such as $W_6Se_8L_6$ or $W_6Te_8L_6$ has been reported. The present paper describes the syntheses, characterizations, and structures of the first two new molecular complexes of the tungsten selenide clusters, $W_6Se_8(pip)_6$ and $W_6Se_8(py)_6$.

Experimental Section

Materials. The reagents and products are air and moisture sensitive. Therefore, all manipulations were performed by the use of an inert-atmosphere drybox, a high-vacuum manifold, and Schlenk techniques, unless otherwise stated. W_6Cl_{12} was prepared by literature methods.⁵ Na_2Se was prepared by the reaction of sodium metal and selenium in refluxing tetrahydrofuran with catalytic amounts of naphthalene.¹⁰ All solvents were purified and dried prior to use and then distilled onto 3- or 4-Å molecular sieves and stored under vacuum or a nitrogen atmosphere. Pyridine (Fisher) and piperidine (Fisher) were purified by refluxing over calcium hydride for at least 4 h. Methanol (Mallinckrodt) was dried by refluxing over sodium methoxide.

Physical Measurements. Infrared spectra (4000 – 200 cm^{-1}) were recorded with a Bomem MB-102 Fourier transform infrared spectrometer equipped with CsI optics. Samples were prepared as Nujol mulls and mounted between CsI windows. 1H NMR spectra were collected on a Unity 300-MHz spectrometer with the samples dissolved in deuterated chloroform. XP spectra were collected with a Physical Electronics Industries 5500 multitechnique surface analysis system, and binding energies (BE's) were calibrated with $C 1s$ BE = 284.6 eV.

Chemical Analyses. Chlorine was determined by potentiometric titration with a standardized silver nitrate solution after dissolving the sample in $KOH-H_2O_2$ solution and neutralization. Additional microanalyses for carbon, hydrogen, and nitrogen were obtained from Oneida Research Services.¹¹

Preparation of $W_6Se_8(pip)_6 \cdot xpip$. W_6Cl_{12} (0.250 g, 0.164 mmol) and Na_2Se (0.164 g, 1.31 mmol) were weighed in the drybox and

[⊗] Abstract published in *Advance ACS Abstracts*, November 1, 1995.

- (1) Chevrel, R.; Sergent, M. *Topics in Current Physics*, Fischer, Ø., Maple, M. B., Eds.; Springer-Verlag: Heidelberg, 1982; Vol. 32, Chapter 2.
- (2) Peña, O.; Sergent, M. *Prog. Solid State Chem.* **1989**, *19*, 165.
- (3) Mulhern, P. J.; Haering, R. R. *Can. J. Phys.* **1984**, *62*, 527.
- (4) (a) McCarty, K. F.; Schrader, G. L. *Ind. Eng. Chem., Prod. Res. Dev.* **1984**, *23*, 519. (b) McCarty, K. F.; Anderegg, J. W.; Schrader, G. L. *J. Catal.* **1985**, *93*, 375.
- (5) Zhang, X.; McCarley, R. E. *Inorg. Chem.* **1995**, *34*, 2678.
- (6) Xie, X.; McCarley, R. E. Manuscript in preparation.
- (7) Zhang, X. Ph.D. Dissertation, Iowa State University, Ames, IA, 1991.

- (8) (a) Hilsenbeck, S. J.; Young, V. G., Jr.; McCarley, R. E. *Inorg. Chem.* **1994**, *33*, 1822. (b) McCarley, R. E.; Laughlin, S. K.; Spink, D. A.; Hur, N. *Abstracts of Papers*, 3rd Chemical Congress of North America, Toronto, Ontario, Canada, 1988; American Chemical Society: Washington, DC, 1988. (c) Zhang, X.; Hur, N.; Spink, D. A.; Michel, J. B.; Laughlin, S. K.; McCarley, R. E. Manuscript in preparation.
- (9) Saito, T.; Yoshikawa, A.; Yamagata, T.; Imoto, H.; Unoura, K. *Inorg. Chem.* **1989**, *28*, 3588.
- (10) Thompson, D. P.; Boudjouk, P. *J. Org. Chem.* **1988**, *53*, 2109.
- (11) Oneida Research Services, Inc., Whitesboro, NY.

Table 1. Crystallographic Data for the $W_6Se_8L_6$ Cluster Complexes

	$W_6Se_8(pip)_6 \cdot 8pip$ (1)	$W_6Se_8(py)_6 \cdot 6py$ (2)
chem formula	$C_{70}H_{154}N_{14}Se_8W_6$	$C_{60}H_{60}N_{12}Se_8W_6$
fw	2926.86	2683.99
space group	$I\bar{4}3d$ (No. 220)	$R\bar{3}$ (No. 148)
a , Å	31.150(4)	19.654(2)
c , Å		15.100(5)
V , Å ³	30 225(11)	5051(2)
Z	12	3
ρ_{calcd} , g/cm ³	1.929	2.647
μ , cm ⁻¹	97.62	145.90
radiation (λ , Å)	Mo K α (0.710 69)	Mo K α (0.710 69)
T , °C	-50	-65
R^a	0.0415	0.0295
R_w^b	0.0397	0.0254

^a $R = \sum ||F_o| - |F_c|| / \sum |F_o|$. ^b $R_w = [\sum w(|F_o| - |F_c|)^2 / \sum w|F_o|^2]^{1/2}$; $w = 1/\sigma^2(|F_o|)$.

transferred into a 100-mL Schlenk reaction flask equipped with a water-cooled condenser. By distillation, 40 mL of piperidine was added to the reactants, and the mixture was refluxed for 3–4 days. A tan solid and purple-red solution were separated by filtration. Single crystals of $W_6Se_8(pip)_6 \cdot 8pip$ (1) were grown from a portion of the filtrate by allowing it to stand at room temperature for several days. The solvent was then removed from the filtrate under dynamic vacuum, and after drying overnight *in vacuo*, 0.30 g of dark red powder (74% yield) was obtained. IR (Nujol, cm⁻¹): 1350 (w), 1304 (m), 1261 (m), 1185 (w), 1171 (w), 1082 (w), 1054 (m), 1041 (w), 1019 (s), 976 (s), 935 (w), 868 (s), 805 (ms), W–Se 243 (ms), 223 (w). Anal. Calcd for $W_6Se_8(pip)_6$: C, 16.04; H, 2.94; N, 3.74. Found: C, 16.70; H, 3.24; N, 3.35. A test for chloride was negative. The tan insoluble product obtained by filtration of the reaction mixture was washed with methanol for 2–3 days to remove NaCl, and about 0.18 g of black solid was recovered.

Preparation of $W_6Se_8(py)_6 \cdot xpy$. W_6Cl_{12} (0.250 g, 0.164 mmol) and Na_2Se (0.164 g, 1.31 mmol) were weighed in the drybox and transferred into a 100-mL Schlenk reaction flask equipped with a water-cooled condenser. By distillation, 40 mL of pyridine was added to the reactants, and the mixture was refluxed for 3–4 days. A brown solid and reddish brown solution were separated by filtration. Single crystals of $W_6Se_8(py)_6 \cdot 6py$ (2) were grown from a portion of the filtrate by allowing it to stand at -20 °C for several days. The remainder of the filtrate was evaporated and dried overnight under dynamic vacuum to remove the solvent of crystallization. About 0.21 g of dark brown powder (56% yield) was thus recovered. IR (Nujol, cm⁻¹): 1594 (w), 1348 (w), 1306 (w), 1211 (s), 1168 (w), 1146 (m), 1065 (ms), 1038 (ms), 969 (w), 935 (w), 750 (s), 687 (s), W–Se 254 (ms), 224 (w). Anal. Calcd for $W_6Se_8(py)_6$: C, 16.3; H, 1.36; N, 3.80. Found: C, 15.0; H, 1.42; N, 3.03. A test for chloride was negative. The insoluble product obtained by filtration of the reaction mixture was washed with methanol for 2–3 days to remove NaCl, and about 0.2 g of brown powder was recovered. XPS data were collected for this brown powder in order to obtain evidence for the formation of W metal by disproportionation (see below).

X-ray Structure Determinations

Single-crystal structure determinations were undertaken for both complexes. In each case, a crystal was chosen from material still in contact with the mother solution. The crystal was encased in epoxy cement, attached to the tip of a glass fiber, and immediately inserted into the low-temperature nitrogen stream of the diffractometer for data collection. The cell constants were determined from 25 randomly located and centered reflections. The structures were solved by direct methods using SHELXS¹² and refined on F by full-matrix, least-squares techniques with the TEXSAN package.¹³ Pertinent crystallographic data are listed in Table 1.

Table 2. Atomic Coordinates and Equivalent Isotropic Thermal Parameters (Å²) for the Non-Hydrogen Atoms of $W_6Se_8(pip)_6 \cdot 8pip$

atom	x	y	z	B_{eq}^a
W(1)	0.2500	0.31382(5)	0.0000	3.72(4)
W(2)	0.30858(3)	0.37601(4)	-0.01689(3)	3.84(3)
Se(1)	0.2887(1)	0.4331(1)	-0.0727(1)	4.73(8)
Se(2)	0.2910(1)	0.31652(9)	-0.07151(9)	4.62(8)
N(1)	0.2500	0.2411(3)	0.0000	4.7(8)
N(2)	0.3801(8)	0.380(1)	-0.031(1)	8.3(9)
N(3)	0.228(1)	0.026(2)	0.133(1)	15(1)
N(4)	0.921(2)	0.064(2)	0.330(1)	35
C(11)	0.238(1)	0.217(1)	-0.0361(9)	6.1(7)
C(12)	0.237(1)	0.1701(8)	-0.040(1)	9(1)
C(13)	0.2500	0.149(2)	0.0000	10(2)
C(21)	0.399(1)	0.349(2)	-0.051(2)	13(1)
C(22)	0.445(1)	0.347(1)	-0.069(2)	11(1)
C(23)	0.466(1)	0.388(2)	-0.074(2)	10(1)
C(24)	0.447(1)	0.421(2)	-0.053(2)	17(2)
C(25)	0.396(1)	0.421(1)	-0.044(1)	6(1)
C(31)	0.220(3)	0.072(3)	0.112(3)	22(2)
C(32)	0.175(3)	0.068(3)	0.101(3)	25(2)
C(33)	0.176(3)	0.029(3)	0.063(3)	23(2)
C(34)	0.183(5)	-0.007(5)	0.081(4)	37(5)
C(35)	0.229(2)	-0.006(2)	0.089(2)	16(1)
C(41)	0.926(1)	0.085(2)	0.375(2)	23
C(42)	0.915(2)	0.015(2)	0.335(2)	31
C(43)	0.875(2)	0.006(1)	0.363(2)	25
C(44)	0.880(2)	0.027(2)	0.407(2)	23
C(45)	0.886(2)	0.076(2)	0.402(1)	19

^a $B_{eq} = (8/3)\pi^2[U_{11}(aa^*)^2 + U_{22}(bb^*)^2 + U_{33}(cc^*)^2 + 2U_{12}aa^*bb^* \cos \gamma + 2U_{13}aa^*cc^* \cos \beta + 2U_{23}bb^*cc^* \cos \alpha]$.

$W_6Se_8(pip)_6 \cdot 8pip$ (1). A dark red tetrahedral crystal, with dimensions of $0.5 \times 0.5 \times 0.5$ mm³, was mounted on a glass fiber, and data collection proceeded at -50 °C. Data were collected with an Enraf-Nonius CAD4 diffractometer using Mo K α radiation, over the range $4^\circ < 2\theta < 50^\circ$ for one octant ($-h, -k, -l$), using the ω - 2θ scan technique. Three standard reflections were monitored every 250 reflections and showed no intensity variation over the collection period. A total of 14 212 reflections were collected, of which 2555 were unique ($R_{int} = 0.150$) and 1248 were observed with $I > 3\sigma(I)$. The linear absorption coefficient, μ , for Mo K α radiation is 97.6 cm⁻¹. An empirical absorption correction using the DIFABS program¹⁴ was applied after the structure solution and resulted in transmission factors ranging from 0.75 to 1.16. The data were corrected for Lorentz and polarization effects.

The cubic space group $I\bar{4}3d$ was unambiguously chosen on the basis of systematic absences and intensity statistics. Initial tungsten atom positions were input on the basis of the SHELXS direct methods output. Subsequently, the other non-hydrogen atomic positions were located directly from the electron density difference maps. These atoms were refined with anisotropic thermal parameters, except for those of two free piperidine solvent molecules. Idealized hydrogen positions were calculated and placed in the refinement with C–H distances equal to 0.95 Å and N–H distances equal to 0.86 Å, but their parameters were held constant during subsequent cycles. The asymmetric unit was found to be $W_2Se_2(pip)_2 \cdot 2pip$, where one coordinated piperidine molecule was located on a 2-fold axis ($24d$ site symmetry) and displayed planar conformation. The other piperidine molecules were found in the chair conformation. Refinement of one solvent piperidine molecule (N4, C41–C45) was poorly-behaved; therefore, a rigid group was applied to improve the refinement. The atomic coordinates and equivalent isotropic thermal parameters of the non-hydrogen atoms are given in Table 2. The relatively large B_{eq} values for the heavier atoms (W and Se) and the planar conformation of the two piperidine ligands suggested that this crystal was probably a twin by merohedry.¹⁵ Therefore, refinement of twinning was explored by using the SHELXL-93 program.¹⁶ However, no improvement was obtained by applying this twin refinement. Thus, only the results without the twin refinement are reported here.

(12) Sheldrick, G. M. *Crystallographic Computing 3*; Oxford University Press: Oxford, U.K., 1985.

(13) TEXSAN: *Single Crystal Structure Analysis Software*, Version 1.6c; Molecular Structure Corp.: The Woodlands, TX 77381, 1985 and 1992.

(14) Walker, N.; Stuart. DIFABS. *Acta Crystallogr.* **1983**, A39, 158.

(15) Catti, M.; Ferraris, G. *Acta Crystallogr.* **1976**, A32, 163.

(16) Sheldrick, G. M. SHELXL-93. *J. Appl. Crystallogr.*, in press.

Table 3. Atomic Coordinates and Equivalent Isotropic Thermal Parameters (\AA^2) for the Non-Hydrogen Atoms of $\text{W}_6\text{Se}_8(\text{py})_6 \cdot 6\text{py}$

atom	x	y	z	B_{eq}^a
W(1)	0.07349(2)	-0.01052(2)	0.07258(2)	1.083(7)
Se(1)	0.0000	0.0000	0.2086(1)	1.41(2)
Se(2)	0.13995(5)	-0.02052(5)	-0.07045(6)	1.44(2)
N(1)	0.1637(4)	-0.0213(4)	0.1574(5)	1.8(2)
N(10)	0.5756(5)	0.0585(6)	0.8196(6)	3.3(2)
C(1)	0.1439(5)	-0.0607(5)	0.2340(7)	2.1(2)
C(2)	0.1971(7)	-0.0674(6)	0.2883(7)	2.9(2)
C(3)	0.2751(7)	-0.0292(7)	0.2647(8)	3.2(3)
C(4)	0.2970(5)	0.0137(6)	0.1847(8)	3.0(2)
C(5)	0.2387(5)	0.0155(5)	0.1353(7)	2.2(2)
C(11)	0.6299(6)	0.1327(7)	0.8113(8)	3.6(3)
C(12)	0.6422(6)	0.1740(5)	0.7325(8)	3.0(2)
C(13)	0.5980(6)	0.1380(6)	0.6609(8)	3.2(2)
C(14)	0.5423(6)	0.0586(6)	0.6699(8)	3.2(3)
C(15)	0.5342(6)	0.0233(6)	0.7470(9)	3.1(2)

^a $B_{\text{eq}} = (8/3)\pi^2[U_{11}(aa^*)^2 + U_{22}(bb^*)^2 + U_{33}(cc^*)^2 + 2U_{12}aa^*bb^* \cos \gamma + 2U_{13}aa^*cc^* \cos \beta + 2U_{23}bb^*cc^* \cos \alpha]$.

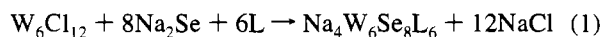
$\text{W}_6\text{Se}_8(\text{py})_6 \cdot 6(\text{py})$ (2). A dark red rhombohedral crystal, with dimensions of $0.35 \times 0.35 \times 0.24 \text{ mm}^3$, was mounted on a glass fiber, and data collection proceeded at -65°C . Data were collected with a Rigaku AFC6R diffractometer using Mo K α radiation, over the range $3^\circ < 2\theta < 55^\circ$ in the hemisphere ($\pm h, \pm k, +l$), using the ω - 2θ scan technique. Three standard reflections were monitored every 150 reflections and showed no intensity variation over the collection period. A total of 4159 reflections were collected, of which 2601 were unique ($R_{\text{int}} = 0.040$) and 1764 were observed with $I > 4\sigma(I)$. The linear absorption coefficient, μ , for Mo K α radiation is 145.90 cm^{-1} . An empirical absorption correction using the DIFABS program¹⁴ was applied after the structure solution and resulted in transmission factors ranging from 0.38 to 1.15. The data were corrected for Lorentz and polarization effects.

The trigonal space group $R\bar{3}$ was unambiguously chosen on the basis of systematic absences and intensity statistics. Initial tungsten atom positions were input on the basis of the SHELXS direct methods output. Subsequently, the non-hydrogen atomic positions were located directly from the electron density difference maps. All non-hydrogen atoms were refined with anisotropic thermal parameters. Idealized hydrogen positions were calculated and placed in the refinement, but their parameters were held constant during subsequent cycles. The asymmetric unit was found to be $\text{WSe}_2(\text{py}) \cdot \text{py}$. The atomic coordinates and equivalent isotropic thermal parameters of the non-hydrogen atoms are given in Table 3.

Results and Discussion

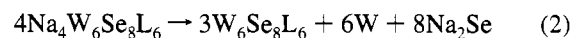
Synthesis of $\text{W}_6\text{Se}_8(\text{pip})_6$ and $\text{W}_6\text{Se}_8(\text{py})_6$. Previous research on sulfide substitution in the $(\text{W}_6\text{Cl}_8)^{4+}$ cluster units (W_6Cl_{12}) showed that NaSH was a good sulfiding agent.⁵⁻⁷ However, NaSH also served as an oxidizing agent for the tungsten during the sulfide substitution. Piperidine and pyridine were used both as solvents with sufficiently high boiling points to conveniently promote the reaction at reflux temperatures and as good ligands for binding in the terminal positions of the W_6Y_8 cluster units, thus stabilizing and solubilizing the cluster complexes.

Ideally, if Na_2Se is used as the selenium source instead of NaSeH , it would lead to the formation of $\text{W}_6\text{Se}_8^{4-}$ or $\text{W}_6\text{Se}_8\text{L}_6^{4-}$ as indicated by eq 1. However, the material recovered from



the filtrate contained the neutral cluster molecule $\text{W}_6\text{Se}_8(\text{pip})_6$ or $\text{W}_6\text{Se}_8(\text{py})_6$ on the basis of spectroscopic analyses (XPS and IR) and X-ray diffraction. The ^1H NMR study of the $\text{W}_6\text{Se}_8(\text{pip})_6$ complex in CDCl_3 provided a spectrum similar to that of $\text{Mo}_6\text{S}_8(\text{pip})_6$.^{8a} No evidence was found for the formation of $\text{Na}_4\text{W}_6\text{Se}_8\text{L}_6$.

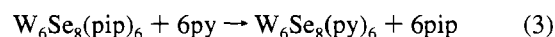
The mechanism for formation of the 20-electron W_6Se_8 cluster unit is still not clear. One possibility is that the 24-electron $(\text{W}_6\text{Se}_8)^{4-}$ unit undergoes disproportionation to form elemental tungsten and $\text{W}_6\text{Se}_8\text{L}_6$ as indicated in eq 2. In the case with L



= pyridine, the insoluble residue isolated after separation of the soluble products $\text{W}_6\text{Se}_8(\text{py})_6$ and NaCl provided XP spectra for both W 4f and Se 3d transitions. The W 4f_{7/2} binding energies (eV) were found at 31.1 (strong), 32.5 (strong), and 34.7 (weak), corresponding to W metal, WSe_2 , and WO_3 , respectively. The last is regarded as only a surface impurity. Thus it appears that some elemental tungsten is formed when the reaction is conducted in pyridine. For the reaction conducted in piperidine, the similarly recovered residue provided XPS data with only one W 4f_{7/2} peak at 32.5 eV. This corresponds most closely to WSe_2 with W 4f_{7/2} at 32.3 eV determined on our spectrometer. Apparently, some WSe_2 results from the reactions in both solvents. Formation of WSe_2 could occur by further disproportionation of the tungsten in the $\text{W}_6\text{Se}_8(\text{amine})_6$ compounds or possibly through oxidation by the amines or methanol, with liberation of H_2 .

Although the primary goal was the preparation of the $\text{W}_6\text{Se}_8\text{L}_6$ cluster complex, the possibility of isolating members of the mixed chloride-selenide series $\text{W}_6\text{Cl}_{8-x}\text{Se}_x\text{L}_6$ with $1 \leq x \leq 8$ was also investigated. A series of reactions with differing $\text{Na}_2\text{Se}/\text{W}_6\text{Cl}_{12}$ mole ratios ($\text{Na}_2\text{Se}/\text{W}_6\text{Cl}_{12} = 1, 2, 4, 6, 8$) was attempted in both refluxing piperidine and pyridine. Regardless of the mole ratio used, the isolated product from the soluble fraction exhibited two types of tungsten in the XP spectrum. One type was identified as that in the $\text{W}_6\text{Se}_8\text{L}_6$ cluster unit, whose W 4f_{7/2} binding energy is 30.8 eV, while the second one, with W 4f_{7/2} BE = 32.8 eV, has not yet been definitely identified but corresponds closely to that of W_6Cl_{12} , BE = 32.4 eV. When a higher $\text{Na}_2\text{Se}/\text{W}_6\text{Cl}_{12}$ mole ratio was used, the XP spectrum showed a decreased relative intensity of the band at 32.8 eV. At the $\text{Na}_2\text{Se}/\text{W}_6\text{Cl}_{12}$ mole ratio of 8, the only product isolated from the reaction filtrate was $\text{W}_6\text{Se}_8\text{L}_6$. No evidence for the formation of any mixed chloride-selenide derivatives was noted either by XPS or by examination of crystals recovered from the reaction mixtures by single-crystal X-ray diffraction. These studies suggest that the mixed chloride-selenide clusters undergo more rapid substitution with Se^{2-} than W_6Cl_{12} , and once the selenide substitution is initiated, it leads to rapid, complete substitution.

Ligand-Exchange Reactions. $\text{W}_6\text{Se}_8(\text{pip})_6$ can be readily extracted with neat pyridine to form a red solution. Single crystals of $\text{W}_6\text{Se}_8(\text{py})_6 \cdot 6\text{py}$ were grown from this solution by allowing it to stand at -20°C for several days. Apparently the complete substitution of pyridine for piperidine was achieved, as illustrated in eq 3. Conversion of $\text{W}_6\text{Se}_8(\text{py})_6$ to



the piperidine adduct was also examined. Upon the extraction with piperidine, $\text{W}_6\text{Se}_8(\text{py})_6$ was found to be somewhat soluble and formed a reddish brown solution. However, upon removal of the liquid after 1 day, several characteristic bands of the coordinated pyridine remained in the IR spectrum of the product. These results suggested that bonding between the hexatungsten cluster and pyridine is stronger than the bonding with piperidine.

A similar conclusion was reached in the study of the ligand exchange reactions between pyridine and piperidine in the analogous sulfide clusters $\text{M}_6\text{S}_8\text{L}_6$ ($\text{M} = \text{Mo}, \text{W}$).^{6,8}

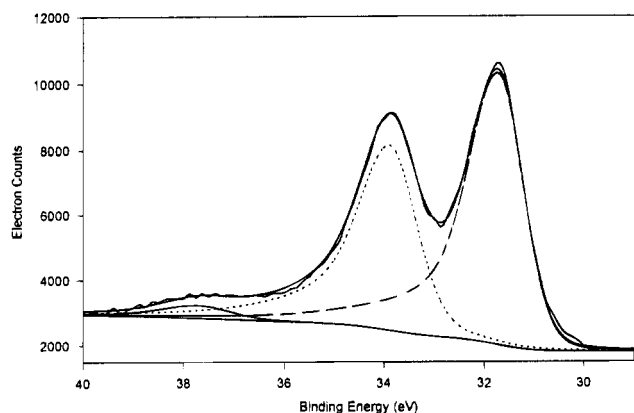


Figure 1. W 4f X-ray photoelectron spectrum of $W_6Se_8(py)_6$. The observed spectrum is given by the upper wiggly solid line, the fitted components are given by the lower dashed line ($4f_{7/2}$) and dotted line ($4f_{5/2}$), and the sum of fitted components is given by the upper smooth solid line.

Table 4. XPS Binding Energies (eV) for the W_6Y_8 Cluster Complexes and Related Compounds^a

compd	W 4f _{7/2}	W 4f _{5/2}	S 2p _{3/2}	Se 3d _{5/2}
$W_6S_8(py)_6$	30.5	32.6	160.6	
$W_6Se_8(py)_6$	30.8	32.9		53.6
$W_6S_8(pip)_6$	30.5	32.6	160.6	
$W_6Se_8(pip)_6$	30.8	32.9		53.7
WS_2	32.7	34.8	162.4	
WSe_2	32.3	34.4		54.6
W_6Cl_{12}	32.4	34.5		
Wmetal	31.4	33.5		

^a Data have been corrected to the C 1s binding energy of 284.6 eV.

X-ray Photoelectron Spectroscopy. XPS was used to obtain tungsten binding energies and gain further information about possible cluster retention or degradation. If decomposition of the cluster unit " W_6Se_8 " did occur to form the thermodynamically favored WSe_2 during any reactions, distinct evidence for this should be found in the resolved W 4f binding energy values. For example, the W 4f XPS of $W_6Se_8(py)_6$ (shown in Figure 1) illustrates that only one type of tungsten is necessary to fit this spectrum. The derived binding energies of 30.8 eV ($4f_{7/2}$) and 32.9 eV ($4f_{5/2}$) are characteristic of the W_6Y_8 unit. For comparison, the W 4f_{7/2} BE for WSe_2 is 32.3 eV. This 1.5 eV difference in BE should make WSe_2 easily detectable when it occurs as an impurity. The XPS binding energies for related compounds are tabulated in Table 4. The materials recovered from the filtrates of the 1/8 (W_6Cl_{12}/Na_2Se) reactions provided XPS that showed W 4f binding energies corresponding only to those of pure $W_6Se_8L_6$ cluster complexes. However, for the insoluble reaction products, as discussed above for the reaction in pyridine, the XPS showed that three different kinds of tungsten were present. Although the component at 31.1 eV was assigned as tungsten metal, we note that the W 4f_{7/2} binding energy for tungsten metal¹⁷ is nearly the same as that for $W_6Se_8(amine)_6$, 31.4 and 30.8 eV, respectively.

Infrared Spectra. The IR bands of compounds **1** and **2** in the mid-IR region (600–3500 cm^{-1}) arise from coordinated piperidine and pyridine, respectively. It is in the far-IR region where two distinctive cluster vibrations occur. The stronger band at about 250 cm^{-1} is assigned as the IR-allowed T_{1u} W–Se

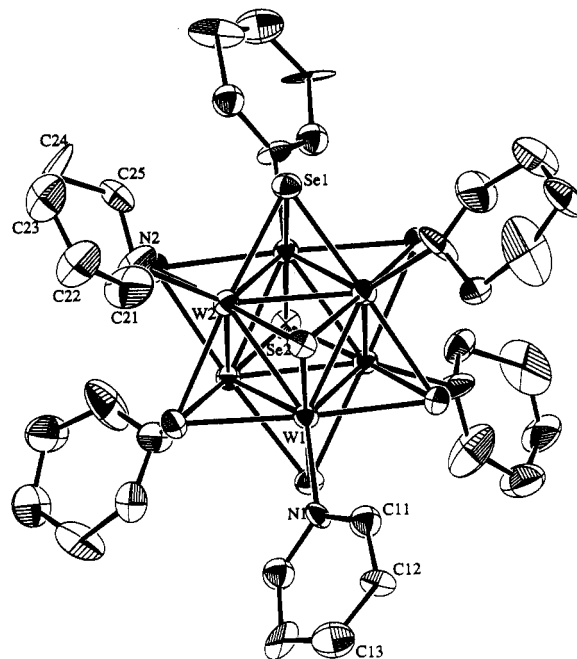


Figure 2. Molecular structure of $W_6Se_8(pip)_6$ in **1**. Thermal ellipsoids are shown at the 25% probability level. Hydrogen atoms have been omitted for clarity.

Table 5. Selected Bond Distances (Å) and Angles (deg) in $W_6Se_8(pip)_6 \cdot 8pip^a$

W(1)–W(2)	2.713(2)	W(1)–Se(1A)	2.567(3)
W(1)–W(2A)	2.668(2)	W(1)–Se(2)	2.569(3)
W(2)–W(2A)	2.687(2)	W(2)–Se(1)	2.563(3)
av W–W	2.689(2)	W(2)–Se(1A)	2.566(3)
W(1)–N(1)	2.26(3)	W(2)–Se(2A)	2.573(3)
W(2)–N(2)	2.28(3)	W(2)–Se(2)	2.575(3)
av W–N	2.27(3)	av W–Se	2.569(3)
W(2)–W(1)–W(2B)	88.87(6)	Se(1B)–W(1A)–Se(1)	175.7(1)
W(1)–W(2)–W(1A)	90.19(5)	Se(2)–W(1)–Se(2B)	176.3(1)
W(2)–W(1A)–W(2B)	90.76(7)	Se(1A)–W(2)–Se(1)	175.7(1)
W(2B)–W(2A)–W(2)	89.97(1)	Se(2)–W(2)–Se(2A)	175.8(1)
av W–W–W	89.95(5)	av Se–W–Se	175.9(1)
W(2)–W(1)–W(2A)	59.90(3)	Se(1A)–W(1)–Se(2)	88.1(1)
W(1)–W(2)–W(2A)	59.23(3)	Se(1A)–W(1)–Se(2B)	91.7(1)
W(1)–W(2A)–W(2)	60.87(3)	Se(1)–W(2)–Se(2A)	91.7(1)
av W–W–W	60.00(3)	Se(1A)–W(2)–Se(2)	88.0(1)
W(1A)–Se(1)–W(2)	62.69(8)	Se(1)–W(2)–Se(2)	90.0(1)
W(2)–Se(1A)–W(2A)	63.18(8)	Se(1A)–W(2)–Se(2A)	90.0(1)
W(1)–Se(1A)–W(2)	63.81(8)	av Se–W–Se	89.9(1)
W(1A)–Se(2A)–W(2)	62.52(8)	Se(1)–W(1A)–N(1A)	92.13(7)
W(1)–Se(2)–W(2)	63.65(8)	Se(2)–W(1)–N(1)	91.87(7)
W(2)–Se(2A)–W(2A)	62.92(8)	Se(1A)–W(2)–N(2)	90.4(8)
av W–Se–W	63.13(8)	Se(2)–W(2)–N(2)	96.9(8)
		Se(2A)–W(2)–N(2)	86.8(8)
		Se(1)–W(2)–N(2)	93.6(8)
		av Se–W–N	91.9(7)

^a Equivalent atoms A and B were generated by symmetry transformations: A, $1/4 - z, 3/4 - y, 3/4 + x$; B, $1/2 - x, y, -z$.

stretching modes. The tungsten sulfide analogues, $W_6S_8(amine)_6$, exhibit similar T_{1u} W–S stretching bands at 376 cm^{-1} . The reduction from 376 to 250 cm^{-1} is about that expected on the basis of the reduced masses. The second band at 223 cm^{-1} must arise from another set of T_{1u} modes involving either W–W or W–N stretching or W–Se bending vibrations. However, this second band also occurs in the spectra of the $W_6S_8L_6$ complexes and the complexes with S- or P-donor ligands. Thus, a reasonable assignment of this band would be as the T_{1u} W–W stretching modes.

X-ray Structure Determinations. Both of the molecular complexes reported here contain the hexatungsten cluster unit

(17) A sample of tungsten metal prepared in this laboratory gave W 4f_{7/2} BE = 31.5 eV on the spectrometer described in the Experimental Section. This compares with a reported value of 31.4 eV in: *Handbook of X-Ray Photoelectron Spectroscopy*; Perkin-Elmer Corp.: Eden Prairie, MN, 1992; p 173.

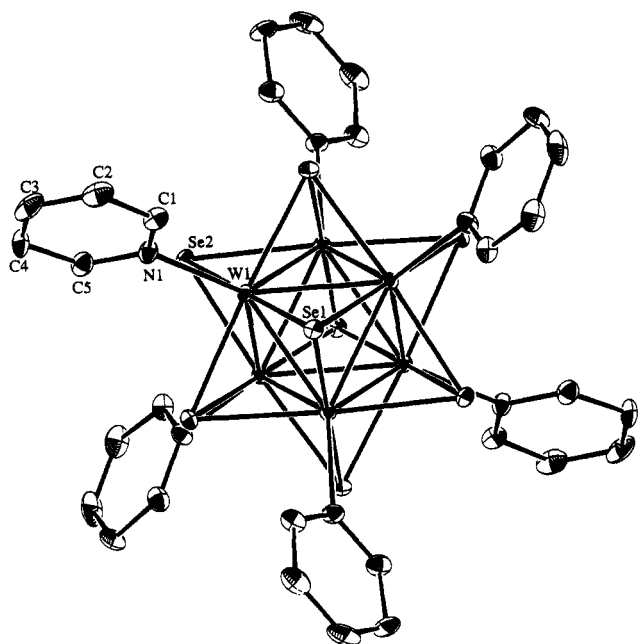


Figure 3. Molecular structure of $W_6Se_8(py)_6$ in **2** as viewed approximately along the $\bar{3}$ axis. Thermal ellipsoids are shown at the 35% probability level. Hydrogen atoms have been omitted for clarity.

$W_6Se_8L_6$. This cluster unit can be viewed as an octahedron of tungsten atoms with eight triply-bridging selenium atoms capping the octahedral faces. Each tungsten also possesses an additional terminal coordination site located at the vertex of the octahedron, which is occupied by the nitrogen-donor ligands.

The cubic $W_6Se_8(pip)_6 \cdot 8pip$ crystallizes in the space group $I\bar{4}3d$ with 12 molecules per unit cell. The W_6Se_8 cluster unit is centered on a $\bar{4}$ position ($12a$ site symmetry). A diagram of the cluster is shown in Figure 2. The piperidine ligand in the chair conformation coordinates to the tungsten atom such that the W–N bond occupies the equatorial position on the N atom. Selected bond distances and bond angles are listed in Table 5. From this table, it can be seen that the deviations from strict octahedral symmetry are quite small. The average bond distances (\AA) and maximum deviations are as follows: W–W, 2.689(2) average, 0.023; W–Se, 2.569(3) average, 0.006; W–N, 2.28(3) average, 0.01. In comparison, the sulfide analogue, $W_6S_8(pip)_6 \cdot 7pip$, crystallizes in the tetragonal space group $I4$ with 8 molecules per unit cell.⁶ It is notable that the average W–W bond distance of 2.659 \AA in $W_6S_8(pip)_6$ is slightly shorter than that of 2.689 \AA for $W_6Se_8(pip)_6$. Both the size of the chalcogen atom and electronic effects must be involved to give this result. EHMO calculations¹⁸ suggest that the W–W overlap populations are higher for the W_6Se_8 cluster than for the W_6S_8 cluster, in spite of the longer W–W distance in the former.

The average W–Se distance of 2.569(3) \AA is much longer than the average W–S distance of 2.461(3) \AA for $W_6S_8(pip)_6$. In order to obtain a value for the covalent radius of W with nonmetallic atoms, the Pauling radius of S, $r(S) = 1.05$ \AA , is subtracted from the average W–S distance to obtain $r(W) = 1.41$ \AA . Applying the latter value to estimate the W–Se distance [$r(W) + r(Se) = 1.41 + 1.17 = 2.58$ \AA] produces a value that is very close to the experimental value, 2.57 \AA . The average W–N distance of 2.28(3) \AA in these selenide clusters is also close to the average values found for the sulfide clusters, 2.31(3) \AA .

$W_6Se_8(py)_6 \cdot 6py$ crystallizes in the trigonal space group $R\bar{3}$ with 3 molecules per unit cell. The W_6Se_8 cluster unit is

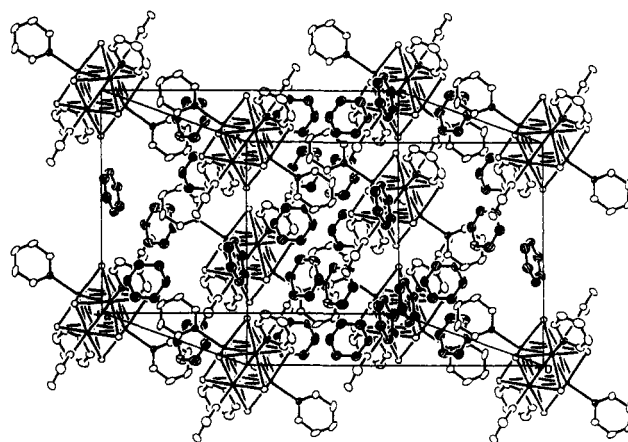


Figure 4. Packing diagram for $W_6Se_8(py)_6 \cdot 6py$ (**2**). Thermal ellipsoids are at the 50% probability level. The carbon atoms in the uncoordinated pyridine solvent molecules are shown as striped ellipsoids and the corresponding nitrogen atoms are shown as shaded ellipsoids.

Table 6. Selected Bond Lengths (\AA) and Angles (deg) in $W_6Se_8(py)_6 \cdot 6py^a$

W(1)–W(1B)	2.6984(6)	W(1)–Se(1)	2.578(2)
W(1)–W(1C)	2.6891(9)	W(1)–Se(2)	2.582(1)
av W–W	2.6938(8)	W(1)–Se(2C)	2.580(1)
		W(1)–Se(2D)	2.572(1)
		av W–Se	2.578(1)
W(1)–N(1)	2.281(7)		
C(1)–C(2)	1.39(1)	N(1)–C(1)	1.34(1)
C(2)–C(3)	1.37(1)	N(1)–C(5)	1.32(1)
C(3)–C(4)	1.41(2)		
C(4)–C(5)	1.38(1)		
W(1C)–W(1A)–W(1D)	60.00(1)	W(1)–W(1D)–W(1A)	90.00(2)
W(1)–W(1B)–W(1C)	59.89(1)	W(1B)–W(1)–W(1D)	90.00(2)
W(1C)–W(1)–W(1D)	60.23(2)		
av W–W–W	60.04(1)	Se(1)–W(1)–Se(2C)	89.52(2)
		Se(1)–W(1)–Se(2D)	89.70(3)
W(1)–Se(1)–W(1B)	63.12(4)	Se(2C)–W(1)–Se(2)	90.18(3)
W(1)–Se(2)–W(1C)	62.90(3)	Se(2D)–W(1)–Se(2)	90.36(3)
W(1)–Se(2)–W(1D)	62.79(3)	av Se–W–Se	89.94(3)
W(1)–Se(2C)–W(1B)	63.18(2)		
av W–Se–W	63.00(3)	Se(2)–W(1)–N(1)	92.7(2)
		Se(2C)–W(1)–N(1)	90.9(2)
Se(1)–W(1)–Se(2)	176.05(3)	Se(2D)–W(1)–N(1)	90.8(2)
Se(2D)–W(1)–Se(2C)	176.51(3)	Se(1)–W(1)–N(1)	93.0(2)
av Se–W–Se	176.28(3)	av Se–W–N	91.8(2)

^a Equivalent atoms were generated by symmetry transformations: A, $-x, -y, -z$; B, $-x + y, -x, z$; C, $y, -x + y, -z$; D, $x - y, x, -z$.

centered on a $\bar{3}$ position ($3a$ site symmetry). A diagram of the cluster unit is shown in Figure 3, and a cell packing diagram of $W_6Se_8(py)_6 \cdot 6py$ is shown in Figure 4. Selected bond distances and bond angles are listed in Table 6. The average W–W and W–Se bond distances are 2.694(1) and 2.578(2) \AA , respectively.

In comparison, the insoluble sulfide analogue, $W_6S_8(py)_6$, crystallizes in the triclinic space group $P\bar{1}$ ($Z = 1$) without any solvent of crystallization.⁵ The solubility of $W_6Se_8(py)_6$ in pyridine is much higher than that of $W_6S_8(py)_6$, so crystals of the former could be obtained directly from the reaction filtrate. For both selenide and sulfide clusters, piperidine adducts are much more soluble in organic solvents than the pyridine adducts. As shown in Figure 4 for **2** and as is also evident in the packing diagram of **1**, the molecules of the cluster complexes are well separated from each other in the lattice. The spaces between are occupied by solvent molecules. In insoluble $W_6S_8(py)_6$, the molecules are packed more closely and the coordinated pyridine molecules are thereby interleaved.⁵

A summary of the average bond distances and bond angles in these four sulfide and selenide complexes is given in Table 7. On the basis of Pauling's relation,¹⁹ $d(n) = d(1) - 0.6 \log n$, the calculated W–W bond distance, $d(n)$, for the W_6Y_8 unit

(18) Xie, X.; McCarley, R. E. Unpublished research.

Table 7. Summary of Selected Average Bond Distances (Å) and Bond Angles (deg) for the $W_6Se_8L_6$ and $W_6S_8L_6$ Cluster Complexes

formula	W-W	W-Y	W-L	Y-W-Y
$W_6Se_8(py)_6 \cdot 6py$	2.6938(8)	2.578(1)	2.281(7)	176.28(3)
$W_6S_8(py)_6^5$	2.6617(2)	2.458(3)	2.255(5)	173.09(7)
$W_6Se_8(pip)_6 \cdot 8pip$	2.689(2)	2.569(3)	2.27(3)	175.9(1)
$W_6S_8(pip)_6 \cdot 7pip^6$	2.6588(3)	2.461(4)	2.31(5)	173.0(2)

with average bond order $n = 20/24 = 0.833$ is 2.677 Å, where $d(1) = 2.630$ Å is used as the W-W single-bond value. The observed W-W distances in the selenide clusters are slightly longer than this calculated distance. The average W-Se and W-N bond distances are essentially identical in these two new selenide cluster complexes after considering the statistical errors. However, the results of the ligand exchange reactions suggested that the W-N bonds in the pyridine adduct were stronger than that in the piperidine adduct. This stronger W-N bonding in the pyridine adduct, however, does not result in any statistically significant difference in the W-W distance that might be expected on the basis of the nature of the donor ligand. The cluster orbitals that are oriented toward the terminal ligands are somewhat antibonding with respect to the W-W bonds of the

cluster. Increased donation of electron density to these orbitals should result in W-W bond lengthening. Besides the longer W-W and W-Se bond distances in the selenide complexes, another notable difference between sulfide and selenide cluster units is the average trans Y-W-Y bond angles. The average trans S-W-S and Se-W-Se bond angles are 173.0(1) and 176.1(1)°, respectively. Thus, the tungsten atom is closer to coplanarity with four selenium atoms than with four sulfur atoms in the W_6Y_8 units.

Acknowledgment. We wish to thank James Anderegg for aid with the XP spectra, Victor Young, Jr., for the data collection of the $W_6Se_8(pip)_6$ structure, and David Scott for aid in collecting the NMR spectra. This work was supported by The U.S. Department of Energy, Office of Basic Energy Sciences, through Ames Laboratory operated by Iowa State University under Contract No. W-7405-Eng-82.

Supporting Information Available: Listings of complete crystallographic parameters, bond distances, bond angles, anisotropic temperature factors, and H atom positions and figures showing unit cell arrangements (13 pages). Ordering information is given on any current masthead page.

IC950650H

(19) Pauling, L. *The Nature of the Chemical Bond*, 3rd ed.; Cornell University Press: Ithaca, NY, 1960; p 400.